frontiers in Earth Science

ORIGINAL RESEARCH
published: 23 February 2021
doi: 10.3389/feart.2020.560081

Geological Structure of the Sylmar Basin: Implications for Slip Distribution Along the Santa Susana/Hospital and Mission Hills Fault System in the San Fernando Valley, CA, U.S.A.

Yuval Levy[1,2]*, *Thomas Rockwell*[1], *Shant Minas*[3], *Alex Hughes*[4] and *Dylan Rood*[5,6,7]

[1]Department of Geological Sciences, San Diego State University, San Diego, CA, United States, [2]Scripps Institution of Oceanography, University of California, San Diego, CA, United States, [3]Applied Earth Sciences, Glendale, CA, United States, [4]Université de Paris, Institut de physique du globe de Paris, CNRS, Paris, France, [5]Department of Earth Science and Engineering, Imperial College London, London, United Kingdom, [6]Earth Research Institute, University of California, Santa Barbara, CA, United States, [7]Department of Earth and Environmental Science & A. E. Lalonde AMS Laboratory, University of Ottawa, Ottawa, ON, Canada

OPEN ACCESS

Edited by:
Nathan Toke,
Utah Valley University, United States

Reviewed by:
Steano Tavani,
University of Naples Federico II, Italy
Reed Burgette,
New Mexico State University, United States

***Correspondence:**
Yuval Levy
uvlevy@gmail.com

Specialty section:
This article was submitted to Structural Geology and Tectonics, a section of the journal Frontiers in Earth Science

Received: *08 May 2020*
Accepted: *27 October 2020*
Published: *23 February 2021*

Citation:
Levy Y, Rockwell T, Minas S, Hughes A and Rood D (2021) Geological Structure of the Sylmar Basin: Implications for Slip Distribution Along the Santa Susana/Hospital and Mission Hills Fault System in the San Fernando Valley, CA, U.S.A. Front. Earth Sci. 8:560081. doi: 10.3389/feart.2020.560081

We developed a forward model using the Trishear module in MOVE to better understand the structure of the northwestern San Fernando Valley and the relationship among the Santa Susana, Hospital, Mission Hills and Northridge Hills faults. This study was motivated by the 1971 San Fernando earthquake and previous work that inferred a high slip rate on the Santa Susana fault, which is in apparent contrast to the lack of significant geomorphic expression of the fault in the Sylmar Basin region. We trenched the Mission Hills anticline from the crest to the base of slope and demonstrate that the Mission Hills anticline is an actively growing fault propagation fold. The associated thrust tip is either deeper than 15 m or sufficiently far to the south that the fault was not encountered in large diameter borings, but the minimum structural relief across the Mission Hills fault since the late Pleistocene is on the order of 37 m, suggesting a minimum uplift rate of 0.5 mm/yr. Our work presents a structural analysis that demonstrates how the Santa Susana fault system evolved in time, with the frontal thrust progressively migrating southward to the Mission Hills fault, and farther south to the Northridge Hills blind thrust. The progression of faulting towards the direction of vergence is compatible with the observed thrust front migration in the western Transverse Ranges of California, and other trust belts around the world.

Keywords: Trishear, Mission Hills Fault, Sylmar basin, Transverse Ranges, Hospital Fault, santa susana fault, Mission Hills Fault, Pleaoseismic trench

INTRODUCTION

Estimating the fault structure, and identifying earthquake sources in tectonically active regions is essential for hazard assessment and reliable ground motion modeling. Two of the most devastating earthquakes in southern California occurred in the San Fernando Valley: the 1971 M_w 6.7 San Fernando and 1994 M_w 6.7 Northridge earthquakes. Each of these events resulted in many millions of dollars in damaged infrastructure along with 60 causalities and thousands were wounded. Both

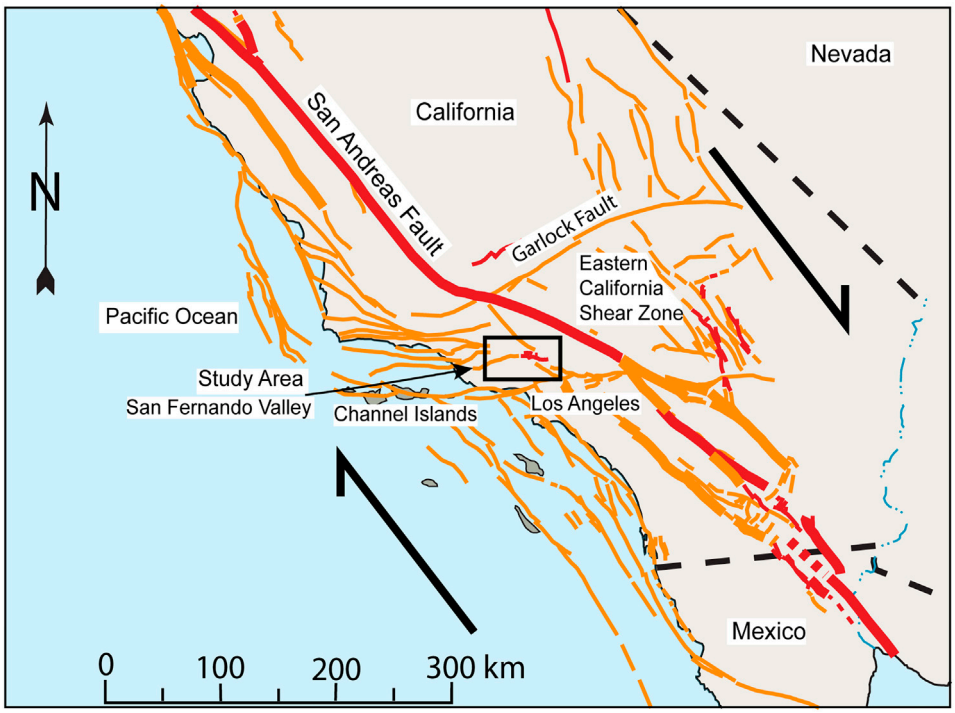

FIGURE 1 | A regional fault map of Southern California, USA. Location of our study area is marked by a black rectangle. The relative motion of the Pacific and North American plates (marked by the arrows) is right lateral and is on the order of 45–50 mm/yr. The Transverse Ranges, located south of the big bend of the San Andreas Fault, accommodate the shortening resulting from the geometry of the big bend. Faults are marked by red and orange lines.

earthquakes exhibited an oblique thrust focal mechanism, but indicated slip on fault planes with opposing dip (Hauksson et al., 1995; Oakeshott, 1975; Whitcomb et al., 1973). The 1971 San Fernando earthquake ruptured the ground surface around the Sylmar basin, which is located in the northern part of the San Fernando Valley (**Figures 1**, **2**) (Oakeshott, 1975). The Northridge earthquake originated on a 35-degrees south dipping thrust at a depth of 19 km on a fault that was unknown prior to the earthquake (Hauksson et al., 1995). No surface rupture was produced as a result of the Northridge earthquake, and the little ground deformation that was reported was located on a secondary structure or due to shaking effects (Woods and Seiple, 1995).

Mori et al. (1995) relocated aftershocks of the two earthquakes and showed the presence of two conjugate planes where the San Fernando plane cuts the Northridge plane and prevents it from reaching the surface. Later work (Tsutsumi and Yeats, 1999; Fuis et al., 2003) suggested that the San Fernando fault zone extends at depth southwestward of the 1971 surface breaks to the Northridge Hills fault and the Mission Hills fault, with the Santa Susana, Hospital and Sierra Madre faults interpreted as upward splays from the underlying décollement. The traces of the Mission Hills and Northridge Hills faults go through major infrastructure and residential areas in the greater Los Angeles region, and thus studying these faults is important.

The subsurface of the northern San Fernando Valley has been extensively studied (Shields, 1977; Davis and Namson, 1998; Tsutsumi and Yeats, 1999; Fuis et al., 2003; Langenheim et al., 2011). However, there are two hypotheses for the formation of the Sylmar basin, which is a small, deep basin at the Northern San Fernando valley. Tsutsumi and Yeats (1999) suggested that the thick accumulation of Plio-Pleistocene sediments in the Sylmar basin is a result of a near-surface expression of the forelimb of the fault propagation fold related to the blind, south-dipping Northridge fault. Langenheim et al. (2011) proposed that the deeply buried Miocene Verdugo-Canyon fault played a role in the formation of the basin. Neither are presented in the literature with satisfactory observations or modeling and are therefore not conclusive. Our structural model, in combination with the observations we review in this paper, demonstrate why the later hypothesis is more defendable.

In current earthquake risk assessments, the Santa Susana fault in the northern San Fernando Valley has one of the highest reported average slip rates in the Transverse Ranges, although with very large uncertainties (Field et al., 2014). The estimated geologic rate for the Santa Susana fault system is 0.5–10 mm/yr and it is based on structural analysis (Huftile and Yeats, 1996; Field et al., 2014). The calculation of the slip rate used magnetic stratigraphy of the fine-grained Saugus and Pacoima strata, with ages of 2.3 and 0.5 Ma for the base and top of the Saugus Formation and base of the Pacoima Formation, respectively (Levi and Yeats, 1993). Petersen and Wesnousky (1994) included the slip rate of the Santa Susana fault (2–8 mm/yr) in their review of active faults in Southern California, and indicated

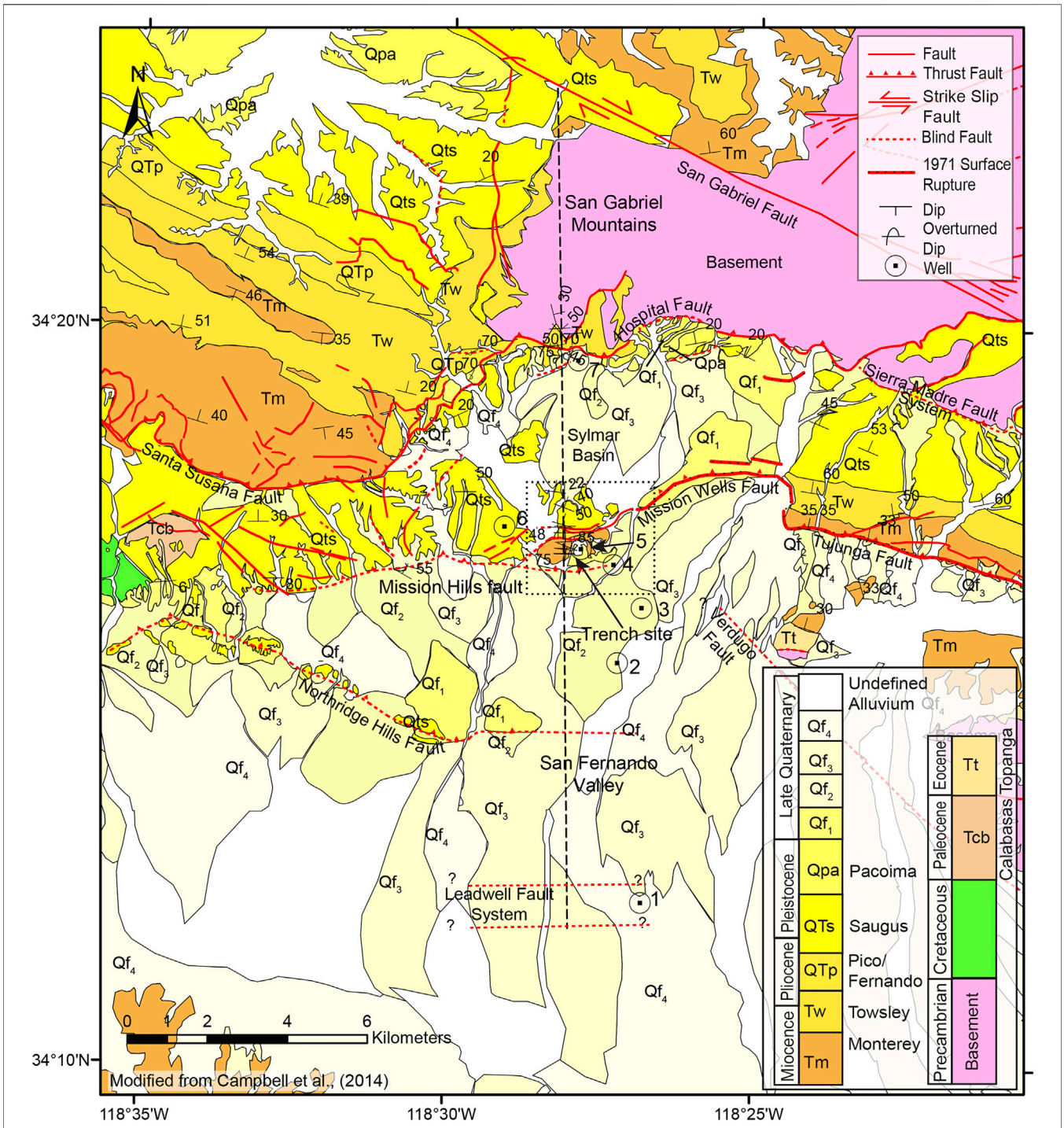

FIGURE 2 | A geological map of the northern San Fernando Valley, modified from Campbell et al., (2014). The stratigraphic column is showing only the mapped units; for a descriptive stratigraphic column of the San Fernando Valley, see **Figure 3**. The location of the cross section in **Figure 4** is marked by the dashed black line. The location of **Figure 5C** is marked by the dashed rectangle. The location of the trench in **Figure 6** is marked by a black arrow.

the lack of reported Holocene movement on the fault. Inverted geodetic and geological data in the western and central Transverse Ranges, using a kinematic model consisting of faults embedded in an elastic crust over an inviscid mantle, yield slip rate estimates of 2–6 mm/yr for the Santa Susana fault (Marshall et al., 2017; Johnson et al., 2020), and Yeats (1987) reported movement on a small segment of the fault during the 1971 earthquake. However, an exploratory trench study (Lung and Weick, 1987) speculated that no slip has occurred on the Santa Susana fault during the past

10,000 years, at least at their excavation site. These reported slip rates are much higher than the erosion rate in the San Gabriel Mountains 0.035–1.1 mm/yr (DiBiase et al., 2010), which is significant when considering the faults geomorphic expression.

Our recent work in the Western Transverse Ranges (Levy et al. 2019) showed how the southward verging system evolved in time. Marshall et al. (2017) summarized the slip rates of major faults in the Western and Central Transverse Ranges, and demonstrated how connectivity and variations in geometry can change the estimated slip rate in the Western Transverse Ranges. In this paper, we present new paleoseismic trenching observation on the Mission Hills fault, and a structural analysis that shows how the Central Transverse Ranges have experienced a similar deformational history to the Western Transverse Ranges during the period of shortening that has been occurring since the Pliocene (Shields, 1977; Dibblee, 1982a; Atwater, 1998). This structural analysis can add to the discussion on slip distribution along the different faults in the northern San Fernando region (e.g., Burgette et al., 2019; Davis, 2016; Numeric Solutions LLC, 2019; Reed et al., 2019), help reduce the large uncertainty on slip rates for some of these faults, and further our understanding of the formation Sylmar basin. Our results and the observations we discuss in this paper suggest that the slip rate of the Santa Susana fault system has been overestimated by prior investigations and that the observed strain might now be accommodated by the Mission Hills and Northridge Hills faults, which lie to the south of the Santa Susana fault.

MATERIAL AND METHODS

Geological Background

The San Fernando Valley is a Neogene basin in the Central Transverse Ranges of Southern California. The San Gabriel mountains that bound the basin in the north were formed by the compressional deformation regime attributed to the big bend of the San Andreas fault, located north of the San Gabriel Mountains and the San Gabriel fault zone (Dibblee, 1982a). A sedimentary and volcanic sequence of Cretaceous through Pleistocene rocks is present beneath extensive late Quaternary alluvium in the San Fernando Valley (Shields, 1977) (**Figure 3**). The Sylmar sub-basin, located at the northern end of the San Fernando Valley (**Figure 2**), is bounded by the Mission Hills and Mission Wells faults in the south and by the segments of the Santa Susana—Hospital—Sierra Madre fault system in all other directions. Gravity modeling suggests that the sediment thickness in the northern part of the Sylmar basin is 5–8 km (Langenheim et al., 2011).

Stratigraphy

In this section, we present a short summary based on previous studies (Shields, 1977; Dibblee, 1991; Tsutsumi and Yeats, 1999; Langenheim et al., 2011; Campbell et al., 2014) of the stratigraphy of the San Fernando Valley (**Figure 3**). We follow the naming convention of Dibblee (1991) and specify additional names where the nomenclature in the literature can be confusing. We then present the relevant structures for our structural modeling and discuss the geological history.

The underlying basement of the San Fernando Valley is composed of Precambrian gneiss and Mesozoic intrusive rocks, which are exposed in the mountains north of the basin. Upper Cretaceous sedimentary rocks are exposed in the western boundary of the basin; the upper contact was encountered in a well (Well #2 in **Figures 2, 4**) but the thickness of these units is unknown. The Cretaceous rocks are predominantly marine sandstone with igneous and metamorphic cobbles (Shields, 1977; Langenheim et al., 2011). Paleocene and Eocene marine clastic rocks overlay the Cretaceous units in angular unconformity.

The Paleocene and Eocene sequence is exposed or penetrated by wells only in the Simi Hills, Chatsworth Reservoir and Horse Meadows Reservoir, which is located west of our focus area (Shields, 1977; Langenheim et al., 2011). The Paleogene Simi Conglomerate of the Calabasas Formation is overlain by the Santa Susana Formation with an angular unconformity. The Santa Susana and Llajas Formations are both siltstone with layers of sandstone. The contact between the Santa Susana-Llajas sequence with the overlying Topanga Formation is an angular unconformity of less than 10° in the San Fernando Valley (Shields, 1977).

The Topanga Formation is of mid-Miocene age and consists of marine clasts and grades eastwards into non-marine beds at the base. The middle units include extrusive basalts and fragmental volcanic rocks interbedded with sandstone. The upper Topanga Formation includes interbeds of marine sandstone and siltstone. The Topanga-Monterey contact in Aliso Canyon is conformable. The Monterey Formation (referred to as the Modelo in some studies) is exposed in Mission Hills (**Figure 2**) and was penetrated by wells in the subsurface throughout the region, with the exception of the northern part of the Sylmar basin. The Monterey Formation is thinly bedded diatomaceous marine shale with chert, siltstone, graded sandstone and laminated sandstone. Analysis of foraminifera indicate a middle- to late-Miocene age (Shields, 1977). Conformably overlying the Monterey Formation is the Towsley Formation, which includes poorly sorted sandstone strata, interbedded with shale and siltstone layers. It is of late-Miocene to early-Pliocene age ranging from 6 to about 3 Ma, where the Miocene-Pliocene boundary is at about 5 Ma (Boellstroff and Steineck, 1975). The contact with the overlying Pico Formation (referred to as Fernando in some studies) is generally conformable. The Towsley Formation is very thick along the Sylmar basin and it thins to the west and southwest. North of the Hospital fault, along its western portion, the lower Pliocene Towsley Formation unconformably overlies gneissic basement rocks.

The marine Pico Formation consists of sandstone and siltstone with layers of conglomerate. Wells in the Mission Hills area indicate two dominant facies within the Pico Formation: an upper, coarse-grained facies and a lower silty facies that may represent a regressive sequence. The Saugus Formation is divided into a lower shallow-water Sunshine Ranch member and an upper non-marine member. The upper member is composed of a coarse-grained sandstone and conglomerate that contains cobbles derived from the San Gabriel Mountains. The upper 9–20 m of the Saugus Formation includes sandstone and shale cobbles derived from the Monterey and Towsley Formations. In the Sylmar Basin, a well penetrated over 3 km of Saugus deposits. The Pacoima Formation overlies the Saugus in several locations and consists of alluvial gravel and sand derived from adjacent mountains to the north.

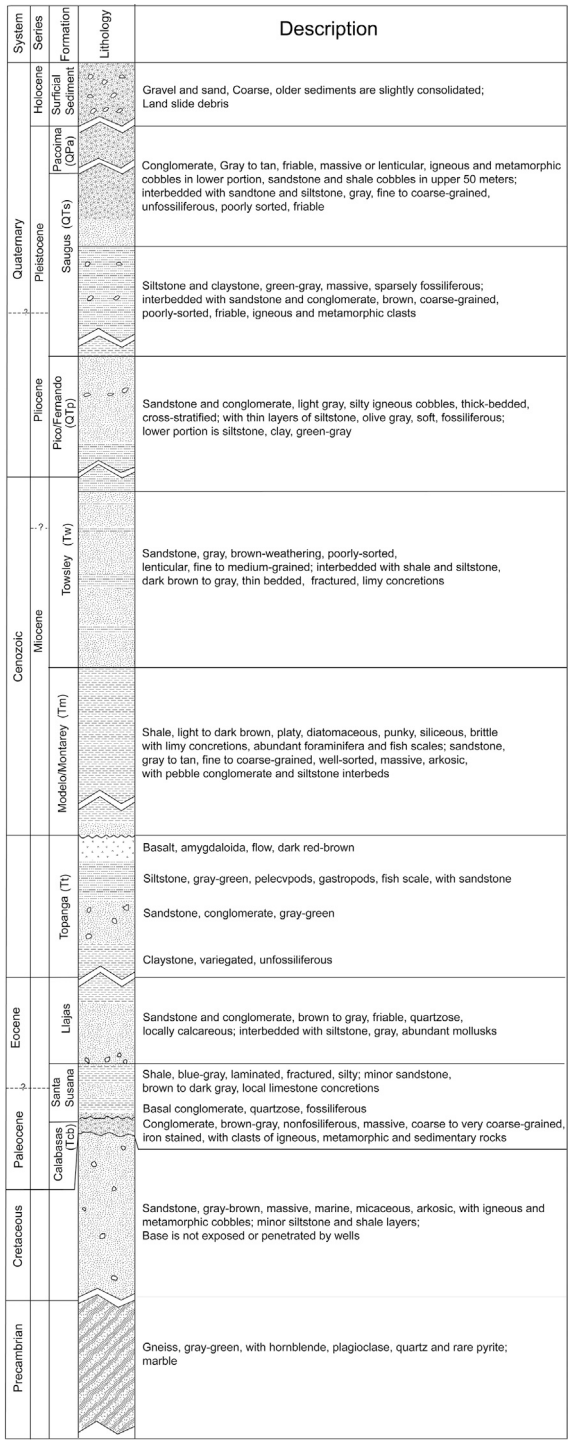

FIGURE 3 | Stratigraphic column (Modified from Shields, 1977) of the geological formations in the northern San Fernando Valley.

Figure 2 presents part of the map by Campbell et al. (2014) who mapped Quaternary units based on geomorphic expression, supplemented by description of the subsurface materials in numerous boreholes from throughout the valley area. Quaternary alluvial fans are presented in stratigraphic order in **Figure 2**, and show the deposition of young alluvial fans occurring south of the Mission Hills fault and that the Santa Susana fault is not producing young alluvium, as expected if the fault has mostly ceased motion and considering the estimated erosion rates of the region (Scott and Williams, 1978).

Structure

The shallow subsurface structure in the San Fernando Valley has been studied extensively (e.g., Shields, 1977; Davis and Namson, 1998; Tsutsumi and Yeats, 1999; Langenheim et al., 2011), but these structural models, with the exception of Davis and Namson (1998) do not attempt to model the deeper underlying structure.

Tsutsumi and Yeats (1999) divided the late Cenozoic faults into three groups, inactive Miocene normal faults, inactive reverse Pliocene faults (pre-Saugus) and Quaternary (post-Saugus) active faults. We focus our discussion to faults relevant to our study area.

The north Leadwell fault system (**Figure 2**) consists of a number of north-dipping normal faults. Langenheim et al. (2011) interpreted a seismic reflection profile with well constraints that shows the Leadwell fault zone offsetting basement and the top of the Topanga Formation just south of the Northridge Hills anticline. They interpret the Miocene to Quaternary units to be offset in reverse sense under the Northridge Hills by the northernmost fault in the system. The subsurface contacts north of the Mission Hills fault seem to be dipping and thickening north towards the fault (Langenheim et al., 2011). In their geological cross section, Langenheim et al. (2011) did not include the reverse sense of slip for the north Leadwell fault zone.

The Hospital fault is located between the Sierra Madre fault system, and the northeastern step of the Santa Susana fault (**Figure 2**). The Hospital fault exhibits reverse sense of motion and places basement or Towsley and Pico Formations in the hangingwall over the Quaternary sediments to the south, bounding the Sylmar basin on the north (**Figure 2**). The Hospital fault slipped a small amount (10–15 cm) during the 1971 earthquake, but this motion has been interpreted as the result of flexural slip as most of the surface deformation was located to the south (Lindvall and Rubin, 2008).

The Santa Susana fault is interpreted as an inverted normal fault (Huftile and Yeats, 1996) based on thickening of Towsley Formation towards the currently uplifted block and its absence from the other side of the fault: such a relation requires basin inversion. The Santa Susana fault is located well up on the hillside with bedrock in both the hanging and footwalls, rather than at the topographic break, indicating deformation and uplift of the footwall block of a deeper fault (Huftile and Yeats, 1996). This is similar to the San Cayetano fault in the Fillmore basin of the Western Transverse Ranges, where a southward propagation of the thrust system has been interpreted for the regional scale (Levy et al., 2019) and locally (Rockwell, 1983; Hughes et al., 2018; Hughes et al., 2020).

The Mission Hills fault is a steeply north-dipping reverse fault penetrated by wells located at the edge of the Mission Hills and its associated narrow anticline (**Figure 2**). The Mission Hills fault

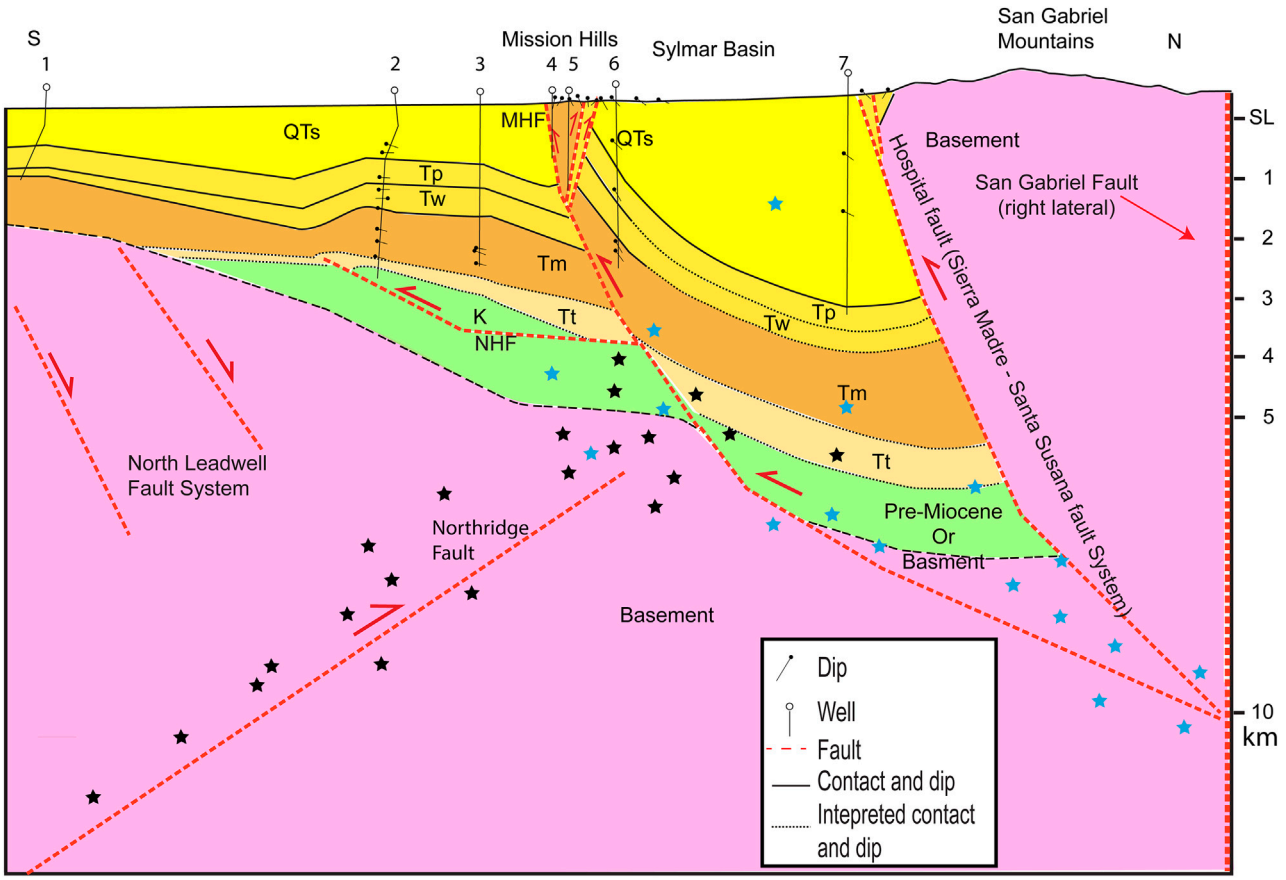

FIGURE 4 | An interpretive geological cross section (location in **Figure 2**) with no vertical exaggeration. Close to the surface the well the section contains observations. The deep part of the section is our interpretation based on the model in **Figures 5, 7** and geophysical observations (Langenheim et al., 2011). The steepened near-surface expression of the Mission Hills fault may result, in part, by motion on the Northridge fault which produced the Northridge earthquake. The black and blue stars are qualitative projections of aftershocks of the 1994 Northridge and 1971 San Fernando earthquakes respectively.

continues west, where it parallels the Santa Susana fault for about 2.5 km to the south of it, along the foothills of the Santa Susana Mountain range. It places Miocene rocks in the hangingwall over late Quaternary sediments in the footwall. An additional associated fault is the Mission Wells fault that ruptured to the surface during the 1971 earthquake (Oakeshott, 1975; Dibblee, 1991), and seems to be stepping north from the Mission Hills fault. There are additional smaller backthrusts and splays associated with the Mission Hills fault. We expand more on the Mission Hills in the following section.

The Northridge Hills fault and its associated anticline are located south of the Mission Hills fault. Baldwin et al. (2000) observed folding of young surficial deposits across the Northridge Hills fault that was interpreted as incremental fold growth produced by fault propagation. The surface expression is very minor, but the fault is observed in the subsurface (Shields, 1977; Baldwin et al., 2000; Langenheim et al., 2011). Shields (1977) and some of the later work (e.g., Langenheim et al., 2011) interpret it as a high angle reverse fault without assigning an actual dip to the fault. However, the cross sections presented in these papers (Shields, 1977; Tsutsumi and Yeats, 1999; Langenheim et al., 2011) show only the upper tip of the fault dipping at about 30° north. It has been suggested that the Northridge Hills fault and the Mission Hills fault merge at depth into a decollement (Tsutsumi and Yeats, 1999; Fuis et al., 2003); this relationship has not been observed but nevertheless seems likely considering the proximity and dips of the Mission Hills and Northridge Hills faults (Fuis et al., 2003).

A study (Fuis et al., 2003) that combined seismic imaging from the lower, middle and upper parts of the crust along with relocated aftershocks for the 1971 and 1994 earthquakes argues for a decollement extending north from the Northridge Hills fault close to the surface to as far north as the San Andreas fault.

Geomorphology

Landscapes experiencing active base level fall, as occurs in virtually all onshore normal and thrust fault terrains, display a common set of landforms that relate to their type of faulting and level of activity (Bull and McFadden, 1977; Keller and Rockwell, 1984; Rockwell et al., 1985; Bull, 2008). Vertical displacements on reverse and thrust faults result in relative base level fall that

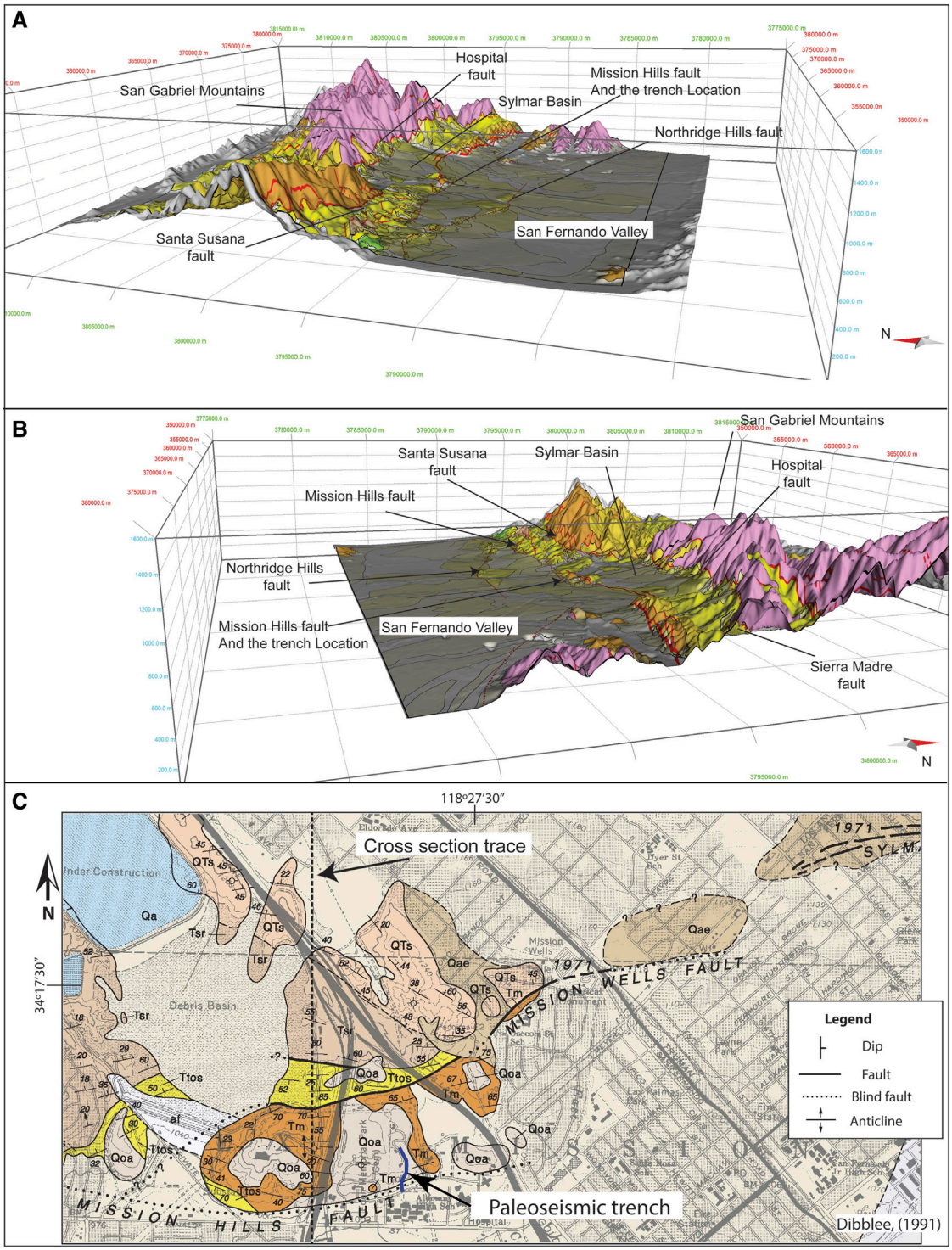

FIGURE 5 | Oblique view from west and east (**A**,**B**, respectively) of the geological map in **Figure 2** projected on a Digital Elevation Model (DEM) with a vertical exaggeration of 5. The young alluvium is almost entirely being deposited south of the Mission Hills fault. The Sylmar Basin is higher in elevation than the San Fernando Valley, which suggests it is being uplifted by an underlying thrust. In caption **C**: enlarged geological map (Dibblee, 1991) of the Mission Hills and trench site area.

invokes incision in the uplifted regions and deposition along the mountain front (Bull, 2008).

Bull and McFadden (1977) and Bull (1977) used a three-part classification to identify tectonically active mountain fronts and to determine spatial patterns of late Quaternary deformation in Southern California. The mountain front class assignment is dependent on a number of factors in addition to uplift rate. These include the hardness or erodibility of the hanging wall

rock, local and regional climate, vegetation type and density (a by-product of climate) and related factors (Bull, 2008). Class 1 thrust fronts are documented worldwide and generally require uplift rates in excess of 1 mm/yr (Keller and Pinter, 1996). Typical landforms along rapidly uplifting mountain fronts (class 1 front) are alluvial fans with fan-head deposition, presence of fault scarps along the front, low range-front sinuosity, low valley and height/valley width (Vf) ratios because most of the stream power is devoted to incision (Bull, 2008). The fault generally produces alluvium from erosion of the hangingwall, and overrides the alluvium in the footwall. For mountain fronts with low uplift rates, stream power and critical power (Bull, 1979) is matched for significant periods of time such that a substantial amount of stream power is used for incision into the downthrown block, resulting in fan-head incision, more sinuous mountain fronts due to lateral cutting, higher Vf ratios and in many cases, the lack of young fault scarps along the range front (class 2 front) (Bull, 2008). Stable tectonic environments (no base level fall) are typified by landforms that represent very low-energy environments where erosion is balanced with the lack of relative uplift. Stream power and critical power are balanced over long time periods to transport the meager amount of sediment supplied from the drainage basins, with the formation of broad pediments (class 3 front) (Bull, 2008).

The Santa Susana thrust fault displays characteristics of a class 2 front. Strands of the fault crop out along the hillslope with no apparent young alluvium in the footwall below the fault, which implies that the rate of erosion exceeds the rate of slip. The alluvial fans along the range front are old and all are incised (fan-head incision) and the younger alluvium is deposited to the south (**Figures 2, 5**), indicating that the uplift front has migrated southward. There is an obvious lack of young scarps associated with the surface traces of the fault, leading previous workers to suggest a complete lack of Holocene activity (Oakeshott, 1975). All of these characteristics indicate either a very low slip rate or that the fault has ceased activity altogether.

Southward propagation of the locus of deformation has been documented in other parts of the Transverse Ranges: in the Western Transverse Ranges west of the Santa Susana fault system (Rockwell, 1983; Hughes et al., 2018; Levy et al., 2019; Hughes et al., 2020), and the central Sierra Madre system to the east of it (Burgette et al., 2019). Previous work on the Mission Hills and Northridge Hills faults, located south of the Santa Susana and Hospital faults (**Figure 2**), are estimated to be slipping at rates of 0.65–1 mm/yr and 0.35 mm/yr, respectively (Tsutsumi and Yeats, 1999). The reverse slip on the Mission Hills and Northridge Hills faults post-dates the inception of reverse slip on the Santa Susana fault (Tsutsumi and Yeats, 1999) and therefore could be the southern extension of the Santa Susana fault system (Fuis et al., 2003).

Geological History

Levy et al. (2019) demonstrated how a regional understanding of the evolution of geologic structure is important when constraining forward structural models. Therefore, a discussion of the geological history is warranted before presenting the forward structural model.

The Transverse Ranges accreted its basement rocks by subduction during the Late-Jurassic and into the Cretaceous (Dibblee, 1982a). In the Mesozoic and Early Cenozoic, the Transverse Ranges occupied the forearc region of a subduction complex collecting continental shelf sediments (Atwater, 1998). The Farallon plate was subducted under the North American plate since at least the Cretaceous and maybe earlier (Liu et al., 2008). The Cretaceous period in the San Fernando Valley appears to represent a period of northwestward flow of sediments from a granitic provenance (Shields, 1977). The Paleocene-Eocene aged units containing basal conglomerates overlies the Cretaceous with an angular unconformity, indicating a period of deformation and erosion close in time to the deposition of the Paleocene-Eocene formations (Shields, 1977). Deposition of the Paleocene-Eocene in the San Fernando Valley occurred in a shelf-environment with sediments flowing west (Shields, 1977).

During the Oligocene, the Pacific plate made contact with North America (Atwater, 1998), and the tectonic regime in the Western Transverse Ranges changed as the San Andreas transform plate boundary evolved over time (Crowell, 1979; Wright, 1991). Oligocene units, such as the Sespe and Vaqueros formations exposed in the Western Transverse Ranges (Dibblee, 1982a; Dibblee, 1982b) are missing in the San Fernando Valley (Tsutsumi and Yeats, 1999). The Global lowering of the sea level (Miller et al., 2005) probably exposed the surface at the northern San Fernando Valley and unlike other nearby localities in Southern California, it did not accumulate sediments, or that these sediments have been removed (Nilsen, 1984).

Early in the Miocene, subsidence and extension with some form of rotation began in the Transverse Ranges region (Nicholson et al., 1994; Schwartz, 2018). Either a spreading ridge associated with continued subduction (Tennyson, 1989) or the evolving transform plate boundary (Crowell, 1979), along with the associated northward migration of the triple junction (Furlong and Schwartz, 2004), caused this extensional tectonic regime. The presence of the volcanics in the lower to middle Miocene Topanga Formation, the transition to deep marine sedimentation later in the Miocene, and normal faulting during that period support the model of a regional transtensional tectonic regime during the Miocene in the Transverse Ranges and other regions in Southern California (Wright, 1991; Atwater, 1998; Ingersoll, 2001).

The angular unconformity between Eocene and Miocene rocks west of Mission Hills (Shields, 1977) might imply that tilting or folding occurred during that time period. The observation of thickening of the Miocene formations northward suggests that the normal faulting continued during the deposition of these units. The Leadwell fault zone was active at least until deposition of the middle Monterey/Modelo strata, and could have been reactivated as a reverse fault during the Late Pliocene (Langenheim et al., 2011). The Santa Susana fault was active as a normal fault during the Miocene and was reactivated as a reverse fault in the Pliocene (Huftile and Yeats, 1995). Additional normal faulting that extends north from the

Leadwell system cannot be ruled out. Furthermore, it is likely that either the Mission Hills fault or some other fault at depth was active during the Miocene as a normal fault and contributed to the formation of the Sylmar basin, based on its thick accumulation of Miocene strata.

Analysis of the provenance of the Monterey/Modelo Formation and of the subsidence during the Late Miocene suggests that the submarine fans depositing sediments during this period originated from the unroofing of the San Gabriel block. This implies that the San Gabriel Mountains were a topographic high during that time (Rumelhart and Ingersoll, 1997). This observation helps explain the unconformity between Late-Miocene or Early-Pliocene units and the basement that is located just north of the Hospital fault along its western portion (**Figure 2**).

During the Pliocene, the tectonic regime changed to transpression as the big bend of the San Andreas plate boundary evolved (Crowell, 1979; Wright, 1991; Atwater, 1998; Ingersoll, 2001). Reverse faulting initiated prior to the deposition of the Saugus Formation by a number of both south and north dipping faults, including the Santa Susana fault (Tsutsumi and Yeats, 1999). A recent report on the seismic hazard in the Aliso Canyon gas storage facility (Numeric Solutions LLC, 2019) suggests that the slip on the Santa Susana fault might have started earlier than suggested by Tsutsumi and Yeats (1995). This report (Numeric Solutions LLC, 2019) also suggests that the rate might be higher and increases the range of estimated slip rates, but for the purpose of hazard evaluation, applies the average rate. The initiation of the Mission Hills and Northridge faults was interpreted to be post-base of Saugus by Tsutsumi and Yeats (1999) based on the constant thickness of the Pico (Fernando) Formation on both sides of the fault. Well data indicate a relatively constant thickness of the Pico Formation across the Mission Hills fault (Langenheim et al., 2011). Tsutsumi and Yeats (1999) estimated 1700–2300 m of total slip on the Mission Hills fault based on dip separation of geological contacts.

South of Mission Hills a number of low hills and folding of the subsurface mark the propagation anticline of the Northridge Hills fault (Shields, 1977; Tsutsumi and Yeats, 1999; Langenheim et al., 2011). The small size of the related folds and the small topographic expression suggest that the total amount of slip on this fault is not very large. The two faults are assumed to connect at depth (Davis and Namson, 1998; Tsutsumi and Yeats, 1999) despite the lack of direct observation (Langenheim et al., 2011).

The observations of thickening of Miocene strata southward and the observed offset through the Leadwell fault system suggest that the formation of the Sylmar basin initiated during the Miocene as an extensional or transtensional basin. In addition, it is likely the case that that the Mission Hills fault may represent an inverted normal fault, as it bounds the Sylmar basin from the south with thickened Miocene in the hangingwall of the fault. Past interpretations explain the presence of the basin as a result of two thrusts on opposite sides, the north dipping Hospital fault from the north side and the south dipping Northridge fault at 12 km depth in the south of the basin. This interpretation requires the regional subsidence rate to be very high everywhere in San Fernando Valley, with thrusts or reverse faults compensating for the vertical motion, with the exception of Sylmar basin. However, the Sylmar basin itself is higher in topographic elevation than the San Fernando Valley south of Mission Hills (**Figure 5A**), and streams incise the rising hangingwall block. These observations clearly indicate that the Sylmar basin is being uplifted at a faster rate than the San Fernando Valley, which contradicts the two opposing thrusts interpretation. In addition, these observations support the idea of connectivity of the north dipping faults at depth. The observed topographic relief in combination with the younger age of initiation for reverse slip on the Mission Hills and Northridge faults support an interpretation of an evolving fault system that is propagating south. We use all of these observations in the construction of a forward model, as presented below.

Interpretive Geological Cross-section

We constructed a geological cross section (**Figure 4**) based on observations from geological maps (Dibblee, 1991; Campbell et al., 2014), well interpretations (Shields, 1977; Davis and Namson, 1998), and geophysical studies (Langenheim et al., 2011). The upper part of the section is based on direct observations while the lower part is based on our interpretation. For the interpretation, we conserved thickness where we thought it is appropriate, but we thickened some sedimentary strata northwards toward the San Gabriel mountains. This thickening is observed for some units and is required for accommodating the Sylmar basin's estimated basal depth (Langenheim et al., 2011).

In order for the Northridge Hills fault to be structurally consistent with the observed fold geometry, a flat is required to accommodate the shape of the anticline, therefore we incorporated a similar interpretation to the one made by Davis and Namson (1998) and interpret the north dipping faults as one fault system. The proposed decollement of Fuis et al. (2003) supports the interpretation of deep connectivity as it could be the surface into which the north dipping faults, such as the Santa Susana and Mission Hills fault, may root.

In the geomorphology section, we explained why the Santa Susana fault does not appear to slip anywhere close to the average rate assigned to it in the literature (Petersen and Wesnousky, 1994; Huftile and Yeats, 1996; Field et al., 2014). A plausible explanation for the lack of apparent activity on the Santa Susana fault trend is that the north-dipping faults are part of an evolving thrust system, and that the locus of deformation migrated southward, similarly to what is observed in the western Transverse Ranges (Levy et al., 2019).

Trenching

To test the activity of the Mission Hills fault, which we interpret as one of the currently active surface traces of the Santa Susana fault system based on its geomorphology, we excavated a series of trenches from the crest of the fold to the base of the slope in the only undeveloped property in the area (Located in **Figure 2**).

Age of alluvial deposits—The alluvium exposed in the three trenches at the site fall into one of three broad categories: terrace deposits associated with the strath surface cut across the growing Mission Hills anticline; alluvial fill that thickens in the southern

forelimb of the fold near the base of slope; and young colluvial deposits at the south side of the project site that represent recent colluvial deposition on the south limb of the fold. The soil description (**Table A1**) was described near the crest of the fold where deposits are thickest, and characterizes the minimum age of the terrace alluvium and the uppermost part of the thickened alluvial deposits on the forelimb, but not the young colluvial deposits at the south side of the project area, which are considered Holocene in age based on their lack of significant soil development, dark color and high organic content. The soil age estimate is considered a minimum because the trench was excavated near the top of slope but on a sloping surface, which implies some erosion may have occurred from the site of the trench. Hence, the soil characteristics are considered minimum values in comparison to what they would have been on a completely stable surface.

Soil, in this context, is the weathering profile that develops at Earth's surface over time (Birkeland, 1984; Rockwell, 2000). The expression of a weathering profile is affected by many parameters, including the characteristics of the parent material, the climatic conditions that prevailed during the period of development along with the associated vegetation that was dominant, the amount of surface slope and aspect that may affect surface stability, and the length of time that a stable surface has been exposed to weathering (Rockwell, 2000).

In this study, the parent material for the terrace alluvium is mostly derived from the San Gabriel Mountains and likely began as a sandy gravel based on its clast-supported character; this is expected for a fluvial terrace environment. The thickened older alluvium on the forelimb contains clasts from the San Gabriel Mountains along with some clasts derived from the Monterey Formation and is likely derived principally from the Pacoima Wash drainage system as it is mapped as Pacoima Formation, although the Pacoima is a general term that includes all post-Saugus fluvial and alluvial fan deposits that are not associated with modern drainages. The young colluvium fronting the forelimb is a silty clay loam interpreted to have been derived from erosion off of the forelimb face.

Variations in the climate in the Mission Hills/Los Angeles basin region are well documented: climate was substantially cooler and wetter in the late Pleistocene than today, with conifer forests growing throughout the coastal and inland region until early Holocene time, whereas the climate during the last interglacial was warm and probably drier than today (Huesser, 1978; 2000; and many other studies by the same author). These changes in climate over time are important in understanding and correctly assessing the ages of the alluvial units exposed in the trenches.

Trishear Modeling

In order to test our hypothesis of southward migration of the thrust front, we used Trishear forward modeling (Erslev, 1991) in Move© (Petroleum Experts Ltd., 2018) and applied the same approach used by Levy et al. (2019) of modeling according to the geological history and comparing to the observed geology. Trishear models produce balanced and retro-deformable sections, however in this work we forward model rather than invert a geological model.

A number of assumptions were made in order to simplify the initial conditions and justify the kinematic elements of our model. First, we assume that the stratigraphy prior to the deposition of the Miocene was a layer cake stratigraphy. We know it was not entirely the case from the different unconformities described in the stratigraphy section. However, these units were deposited on a continental shelf so the assumption seems reasonable at first order, and small unconformities would not significantly affect the model results. Further, the pre-Miocene sedimentary units in our cross section are mostly not directly observed, as most wells do not penetrate deep enough. Therefore, we made no attempt to model the deformation of these units, or assess the exact stratigraphic model during the early Miocene. Another assumption is that out of plane motion is negligible. There is a strike slip component, as was observed during the 1971 earthquakes (Whitcomb et al., 1973), but because the dominant sense of motion is dip slip and the stratigraphy does not dramatically vary laterally along the fault, our models will focus on the dip-slip deformation. An additional assumption is that we only model the main faults in the system, but it is important to remember that there may be additional faults, similar to the blind fault that moved in the Northridge earthquake (Hauksson et al., 1995). We do not model back thrusts because slipping faults in different directions can create discontinuities in the model. As we will discuss, we did change the direction of slip but avoided introducing any discontinuities that will make the model's result unbalanced.

The parameters of Trishear in MOVE (Petroleum Experts Ltd., 2018) include: Slip and Propagation/Slip (P/S) ratio, which controls how far the fault tip propagates for a specific slip. The distribution of the trishear zone between the hangingwall and footwall of the fault is controlled by the Trishear Angle Offset parameter. A Trishear Angle Offset of 0.5 places the trishear zone symmetrically between the hangingwall and footwall, distributing fault-related deformation in both. Values of 0 or 1 attach the trishear zone to the footwall or hangingwall, respectively.

In MOVE, it is possible to simulate both homogeneous and heterogeneous trishear deformation (Erslev, 1991) to control how displacement vectors vary across the trishear zone. When the number of Trishear Zones is set to 1, homogeneous trishear will be simulated and displacement vectors will decrease linearly across one trishear zone. Values >1 signify that the main trishear zone should be sub-divided into an equivalent number of trishear zones and that heterogeneous trishear should be used. For heterogeneous trishear, variations in the displacement vectors are calculated across each of the trishear zones and typically results in the greatest displacement change occurring in the central portion of the main trishear zone

RESULTS

Paleoseismic Trenches

The trenches, which are presented as a composite trench in **Figure 6**, exposed folded Miocene Monterey Formation shale near the fold crest, capped by fluvial terrace deposits that fold over

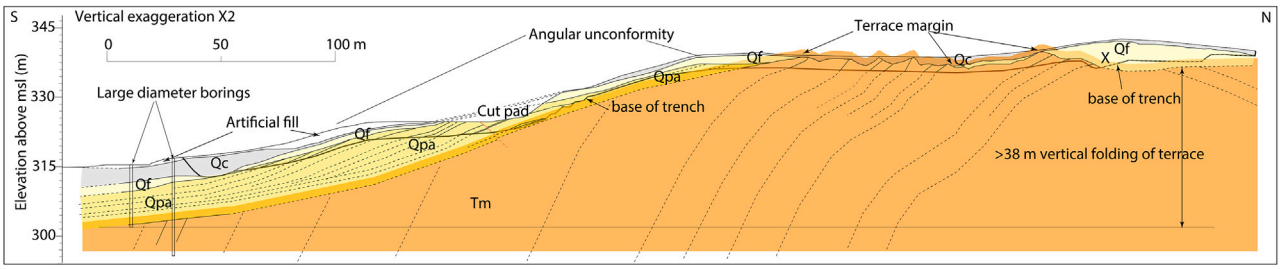

FIGURE 6 | Composite trench log across the front of the Mission Hills anticline. The vertical exaggeration is x2. Bold line shows the base of trench, with the underlying geology inferred from the trench and boring exposures. The soil description in Supplementary Table S1 was completed at the top of the trench where the alluvium was thickest near the fold crest (marked by X). The terrace alluvium and Pacoima alluvium are identical in composition, implying that they are derived from the same source. There is an angular unconformity between the terrace and Pacoima deposits as observed in a portion of the trench, but much of the exposure containing the angular unconformity was removed by cutting of a pad. Qc—colluvium, Qf—fan deposit, Qpa—Pacoima, Tm—Monterey.

the anticline to the base of slope. The fluvial deposits thicken at the base of slope, indicating alluvial fan deposition at the local front of the south verging fault system. The trench was excavated close to the margin of the terrace, and in places cut the margin such that the terrace deposits were not continuously present on the western wall (**Figure 6**). Although not shown here, the terrace deposits were exposed continuously on the eastern wall of the trench as the alluvium thickens eastward into its paleo-channel. At the base of slope, the alluvium is buried by a progressively thickening wedge of colluvium to the southern end of the trench. The colluvium is interpreted to be entirely Holocene in age based on its dark color and high organic content, which should oxidize over time (Rockwell, 1983).

We bored two 60 cm-wide bucket auger holes (**Figure 6**) to test the thickness of the colluvial deposits and to try and penetrate the Mission Hills fault. Instead, we encountered the fluvial alluvium and Pacoima deposits beneath the colluvium, with the alluvium cut across a strath surface on the folded Monterey Formation shale; this provides a marker from which to estimate the minimum structural relief since deposition of the alluvium, as discussed below. It is a minimum because the bucket augers were drilled on the hangingwall and did not penetrate the fault. The equivalent strata on the footwall may be substantially deeper.

The trench excavated into the terrace deposits that cross the crest of the anticline varied in depth from about 1.5 m to nearly 5 m, depending on the depth to Monterey Formation bedrock. The described pedon (Table 1) is in the deepest part of the trench near the anticlinal crest where the alluvium extended to the bottom of the trench; the alluvium was probably thicker to the east, which is now eroded out by the modern channel and adjoining hillslope, so the variations in alluvial thickness are interpreted to result primarily from distance to the paleo-channel wall. That said, we chose to describe the soil at the crest of the fold where erosion should be less than on the fold forelimb.

The terrace surface preserves a 30–40 cm-thick A horizon (37 cm at the description locale) overlying a 1.2–2 m thick, moderately well-developed argillic horizon exhibiting 7.5YR hues and a sandy clay loam texture. There is moderately well developed angular blocky structure, extremely hard dry consistence, and plastic and very sticky wet consistence. Clay film development is strongly expressed with continuous thick clay films on ped faces and in pores, and many moderately thick clay films bridging grains in the matrix. These are common characteristics of gravel-rich late Pleistocene soils in non-arid regions of southern California, as discuss further below.

The argillic horizon grades downward into a transitional horizon, the BC horizon, which grades downward into the Cox horizon below about 3 m depth. The BC horizon exhibits typical 10YR hues, which is likely the initial color of the parent material, and massive to weak subangular blocky structure. This is consistent with the loamy sand texture, soft dry consistence and weakly developed clay film frequency and thickness.

The Soil Development Index (SDI) (Harden, 1982) was applied to the soil description, and the SDI value was compared to dated gravelly, coarse-grained soils in southern California (Rockwell, 1983; Rockwell et al., 1985). The SDI compares the current characteristics of the soil to that of the parent material, which in this case is inferred to have been loose gravelly sand with an initial color of 10YR x/2. The parent material for the A Horizon is assumed to be a loamy silt, as there appears to be a significant aeolian component to that horizon. Based on this, the SDI calculated for this profile is 123 at 380 cm depth, which is the depth used for comparison to the dated Ventura soil chronosequence (Rockwell, 1983) because the SDI calculation is depth dependent. The Maximum Horizon Index (MHI) (Ponti, 1985; Rockwell, 2000) can also be used for comparison to dated soils, and for this profile, a maximum value of 0.76 was calculated.

The Mission Hills soil is most similar to the Q6 soils of Rockwell (1983), which suggests that the age falls in the 40,000 to 90,000 year range. Recalculated SDI values (Rockwell, 1983) for the Merced soil chronosequence of Harden (1982) suggest an older age that is comparable to the Riverbank series, which is correlated to the last interglacial period at about 120,000 years. For comparison, the oldest dated soil in the Cajon Pass chronosequence (McFadden and Weldon, 1987) yielded SDI values around 70–75 for the 55,000 year-old terrace, supporting the older age range. However, in terms of parent material and proximity to the coast, the Ventura chronosequence is the closest match.

However, one factor that supports a late Pleistocene age of the terrace alluvium is the absence of a calcic horizon associated with

the surface soil. Inland Los Angeles Basin region soils, and especially in the San Fernando Valley, experienced the extended dry period of the last interglacial period from about 130 to 115 ka, and perhaps as late as 80 ka, and typically exhibit a stage II to Stage II+ calcic horizon below the Bt and BC horizons. The absence of such a calcic horizon suggests that this soil is younger than 115–130 ka in age. It is possible that such a calcic horizon was leached out during the wetter late Pleistocene, but as a calcic horizon is preserved in last interglacial soils elsewhere in Los Angeles basin (Rockwell; unpublished catalog of dated soil profiles), this is not a satisfactory explanation. Consequently, we infer the likely age of the terrace deposits to be in the 60,000- to 80,000 year range, based on the soil profile characteristics. Considering that the upper part of the soil may be eroded or deflated, this soil age estimate should be considered a minimum, but again, there is no indication that the soil experienced the last interglacial dry period based on the lack of a calcic horizon, and the presence of a thick A horizon and a complete argillic horizon argue against a large amount of erosion.

Trishear Modeling Results

We first tried to model a layer cake stratigraphy and north dipping stratigraphy for the sequence of reverse faults, however these attempts proved to be unsatisfactory. The depth of the sedimentary formations in the Sylmar basin is known to be deep both from wells and as implied by gravity and seismic data (Langenheim et al., 2011). South of Mission Hills, units dip to the north and thicken towards the Sylmar basin. North of Mission Hills, the Quaternary is substantially thicker than to the south. Those observations and our lack of success with simpler models led us to add a period of normal faulting in our forward model. The different stages are presented in **Figure 7**. The first steps simulate the normal faulting that occurred during the Miocene. First, the faults slip from south to north for the normal faulting stage. The model does not allow separate faults to slip at the same time, and because the basin is north of the normal fault system, we chose this direction for the fault sequencing. After slipping the normal faults, we added another layer and repeated this step. This simulates the extension and normal faulting with continued deposition of growth strata. This period of simulated extension is followed by shortening represented by the reverse sense of slip on some faults. For our case, we create a new fault that represents the Hospital fault. However, it is important to mention that the Santa Susana fault west of the Hospital fault is interpreted as a reactivated normal fault (Huftile and Yeats, 1995) and it might be the case for the Hospital fault.

The next step in the model progression is to propagate slip to the Mission Hills fault, forming the anticline and topographic relief as observed in the southern boundary of Mission Hills. In our model, the Mission Hills is a reactivated normal fault but it does not have to be the case, as we will discuss. Then, we slip the Northridge Hills fault which has a very small topographic expression that is related to folding observed in the subsurface: both the fold and the fault have been penetrated by wells. Finally, we slip the Northridge fault at depth. We include the Northridge fault in the model but recognize that the depth of the Northridge fault and lack of subsurface control at those depths makes it impossible to determine when it initiated and how much it has slipped. Due to the lack of apparent structure close to the surface and the fact the fault is known to be active, we decided to include it last and assign a rather small amount of slip on the fault. However, we do recognize that the north dipping fault system and the south dipping Northridge fault are both active.

The model parameters we used are as follows. For each of the Leadwell normal faults we used 500 m of Miocene dip slip, P/S ratio of 1, 1 Trishear zone, and no offset for the Trishear angle. We then offset the Mission Hills fault in a normal sense by 1000 m with a P/S ratio of 1, 1 Trishear zone, and no offset for the Trishear angle and sediment horizon after slipping this fault. We repeated this process 4 times. We then slip the reverse faults from north to south. The parameters we used for the different faults are: 7000 m of slip for the Hospital fault, P/S ratio of 1, 1 Trishear zone, and no offset for the Trishear angle. We applied 3400 m of slip on the Mission Hills fault, a P/S ratio of 1.2, 9 Trishear zones, and 0.6 offset on the Trishear angle. For the Northridge Hills fault, we applied 700 m of slip, a P/S ratio of 1.2, 9 Trishear zones and 0.8 offset on the Trishear angle. The last stage was slipping the Northridge fault at depth by 1000 m with: P/S ratio of 1, 1 Trishear zone, and no offset for the Trishear angle.

Our model results (**Figure 8**) appear to be structurally consistent to the first order with our interpreted cross section and other published cross sections. The presented cross section includes both observations from the surface geology (Dibblee, 1991) a number of wells (**Table A2**) and our interpretation of the deep structure as constrained by our model and geophysical data (Langenheim et al., 2011). The depth of sedimentary units in the basin, folds and general relief are faithfully reproduced by the model. We do not try to match exactly every observed dip, mainly due to the number of steps required for each simulation and the general lack of observations that will determine exact thickness of the formations in the subsurface of the Sylmar basin. Under the back-limb of the Mission Hills anticline there is a significant stratigraphic discrepancy (the area of well number 6). This discrepancy is caused by the Trishear model that conserves the area of the unit, and this can result in extreme local thickness variations. Another discrepancy is in the basin, the exact thickness of units is not reproduced by our model; this flaw is related to the deposition of layers and not the order of faulting. Because matching the thickness of each unit across the model is extremely time consuming, we focused on matching the general thickness of units in the basin.

DISCUSSION

Late Quaternary Activity of the Mission Hills Fault

Terrace deformation—The terrace is cut across Miocene Monterey Formation bedrock and older Pacoima alluvium; the Monterey strata exhibits bedding dips up to ~65° to the south whereas the Pacoima dip as much as 25°. The maximum terrace gradient is about 15°, based on trench observations, which implies that much of the folding occurred prior to formation of the strath terrace, and that there has been 12–14° of additional tilting or folding in the past 60–80 thousand years. Continued late Quaternary folding of the

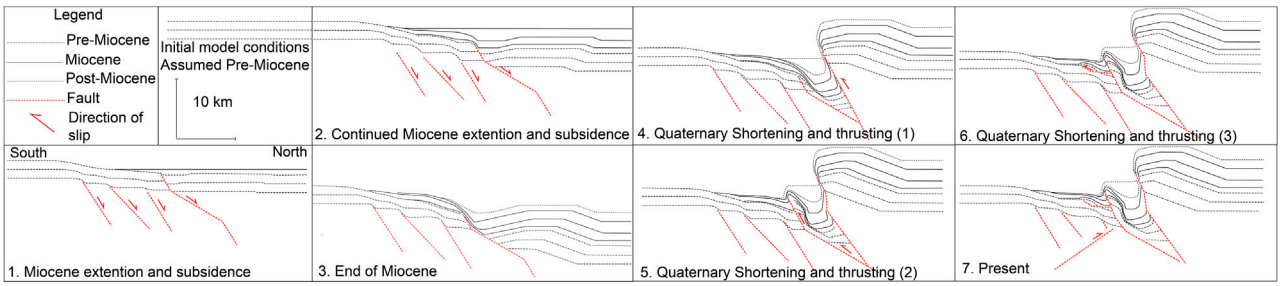

FIGURE 7 | A Trishear forward model presenting the evolution of the Sylmar Basin since the Miocene. Caption descriptions: top left we present a legend and the initial conditions of the model, Pre-Miocene layer are horizontal. 1–3. During the Miocene normal faults (Leadwell fault system and possibly the Mission Hills fault) are slipping due to the regional extension and subsidence. 4. early during the Quaternary, reverse fault (Hospital fault) uplifts the basement in the north. 5. At some point during the late Quaternary the thrust system propagates southward and the normal fault south of the basin is reactivated as a reverse fault (Mission Hills fault), forming the Mission Hills anticline, as discussed in the text the back thrusting is not modeled. 6. Finally, a small amount of slip is distributed farther south on a splay or a new thrust (Northridge Hills fault). 7. During the present conditions a south dipping fault (Northridge fault is slipping at depth), but it is unclear when this fault was initiated. The model illustrates how the observed dips of the pre-Miocene and early Miocene strata south of Mission Hills were formed, and how the thick sedimentary column in the Sylmar basin could have been formed. South is to the left and north is to the right of each caption, as indicated in caption 1.

terrace suggests that some slip on the Mission Hills fault is blind, although we cannot resolve whether the folding has continued into the Holocene.

As we intercepted the strath surface in the bucket auger holes at an elevation of about 300 m, and the terrace lies at about 337 m elevation over the fold crest, we estimate that there has been 37 m of structural relief on the terrace deposit over the past 60–80 ka due to folding alone. This yields a long-term minimum uplift rate of about 0.5 mm/yr. However, as we did not encounter the fault in the auger borings, nor do we know how deep the late Quaternary alluvium is to the south of the frontal escarpment, this calculated rate is likely a gross minimum. Nevertheless, it demonstrates the possibility of slip distribution across the entire system. In this case, the system being the Santa Susana, Hospital and Sierra Madre faults as the initial fault front of the system, and the Mission Hills and Northridge Hills fault as the current fault front of the system. Both might slip in a large earthquake, however, as we mentioned in the introduction, Lung and Weick (1987) did not observe any evidence for activity in the Santa Susana fault during the past 10,000 years: therefore it is hard to explain the inferred high slip rate for the Santa Susana surface trace. We point out that the front along the Mission Hills trace is a class 1 front (Bull and McFadden, 1977; Keller and Rockwell, 1984) in that the modern drainages are incised only in the hanging wall, deposition is at the front, and topography to the north is rising. These characteristics are in marked contrast to that along the surface trace of the Santa Susana fault itself, which argues that the Mission Hills fault is considerably more active.

Propagation of the Santa Susana/Hospital/Sierra Madre Fault System and Formation of the Sylmar Basin

The observations we present in this paper suggest that the Santa Susana fault system propagated southward, as was established for other fault systems along the Transverse Ranges including the Sierra Madre fault (Burgette et al., 2019) and in the Western Transverse Ranges (Levy et al., 2019). Our structural model (**Figures 7**, **8**) demonstrates how a southward propagation of the north dipping fault system could have taken place. Out of sequence thrusting (Butler, 1987) might occur, as well as flexural slip due to the proximity to the Mission Hills fault, but it is clear that to produce the observed geology, the system is evolving and propagating toward the south.

The slip rate used for the Santa Susana fault system in earthquake hazard estimates is based on estimation of displacement from structural cross sections and the age estimates of the Saugus Formation (Field et al., 2014). Levi and Yeats (1993) dated the deposition of the Saugus Formation from about 2.3 to 0.5 Ma based on magnetic stratigraphy and an ash horizon. However, in the eastern Ventura basin, results of a new study (Hughes, 2019)[1] that applied cosmogonic dating methods indicate that the Saugus Formation is significantly older than estimated by Levi and Yeats (1993). Therefore, it is possible that the ages of Quaternary strata in the San Fernando Valley are older than previously estimated. This means that the long-term average slip rate estimates based on the structural cross sections for the Santa Susana fault will decrease. Further, it is possible that the Santa Susana fault is no longer active, at least at a significant rate, considering the geomorphological observations we presented above, and lack of paleoseismic observation to support activity in the last 10,000 years (Lung and Weick, 1987). In any case, if the fault is still active it clearly has a slip rate that is closer to the lower end of previously estimated slip rates (Petersen and Wesnousky, 1994; Huftile and Yeats, 1996; Field et al., 2014).

The recent geodetic and geologic inversions for the region that used kinematic model (Marshall et al., 2017; Johnson et al., 2020)

[1]Hughes, A., Rood, D. H., DeVecchio, D. E., Whittaker, A. C., Bell, R. E.,Wilcken, K. M., et al. (in review). Transient quaternary landscape evolution of the Ventura basin, southern California, quantified using cosmogenic isotopes and topographic analyses. Geological Society of America Bulletin.

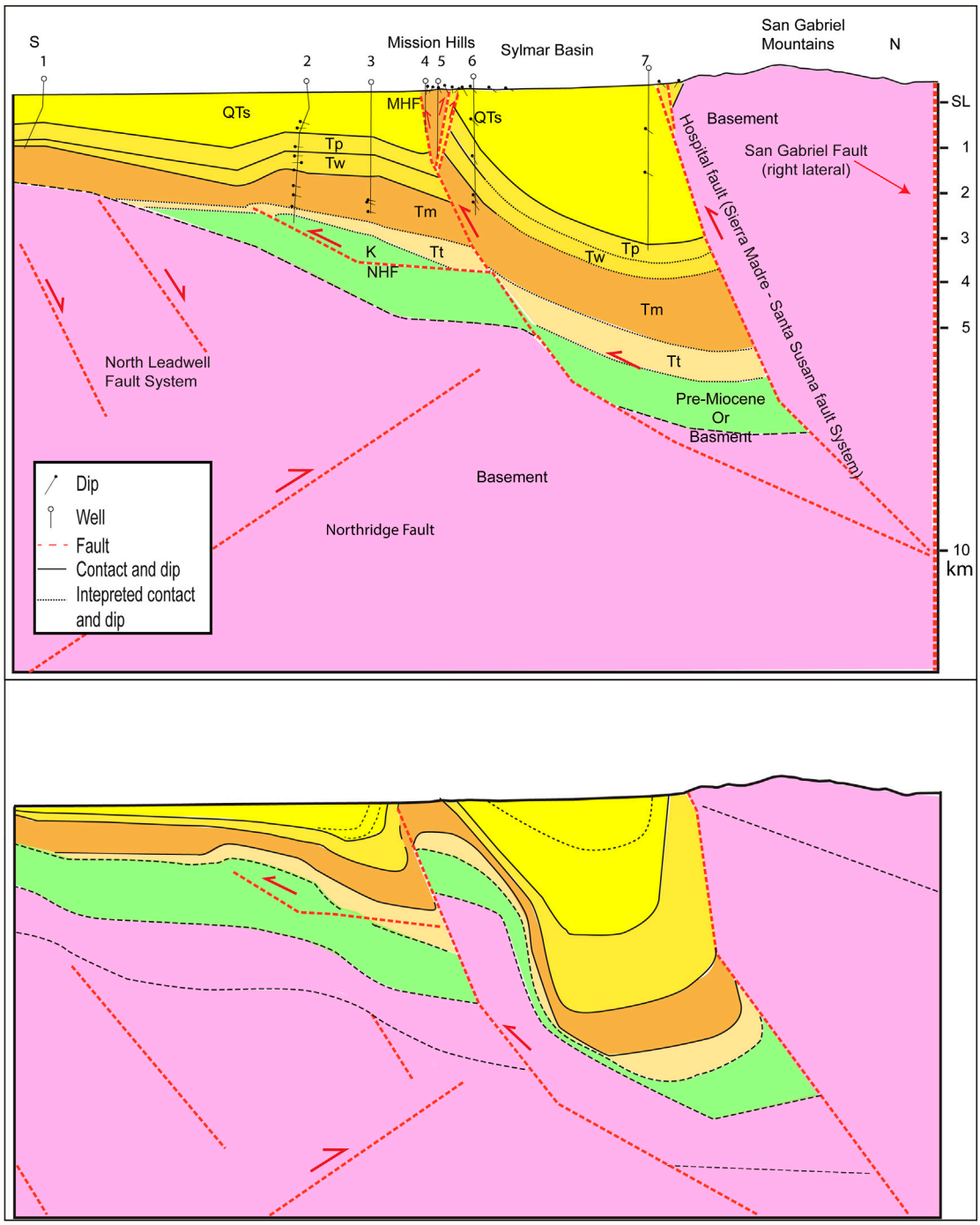

FIGURE 8 | Comparison between the model result and the interpretive geologic cross section (**Figure 2**). To a first order the structures are compatible. For Geological units see the legend in **Figure 2**. To clarify, the Mission Hills fault is blind but the tip might be in the shallow subsurface.

estimate a slip rate of ~0–2 mm/yr for both the Mission Hills and Northridge Hills fault, and 2–6 mm/yr for the Santa Susana. While the slip rate in these kind of models might change significantly due to undiscovered faults (e.g., Northridge), or by applying a different fault geometry (Marshall et al., 2017), they support the idea of distributed slip. However, due to the nature of modeling, the models cannot uniquely resolve which fault carries the dominant amount of displacement because they are closely spaced and only a few kms apart at the surface. Furthermore, our modeling suggests that they merge at depth so the strain accumulation will be a unified signal for all three faults.

The total slip we applied to the Mission Hills fault in our model exceeds previous estimates (Tsutsumi and Yeats, 1999) and implies a higher rate on that fault. Using the same ages of 2.3 to 0.5 Ma as Tsutsumi and Yeats, the slip rate for the Mission Hills fault will be 1.4–6.8 mm/yr. This exceeds prior estimates and could be explained by propagation of slip from the Santa Susana/Hospital fault to the Mission Hills fault. However, it is difficult to determine if our estimates in this model are close to the actual slip of this fault because we do not have a good marker horizon to make an accurate estimate of displacement. Our minimum estimate from the trench is 0.5 mm/yr, but this only accounts for folding and not fault slip, which is likely substantial, nor does it account for how deep the equivalent strata are in the footwall, which was not resolved in this study.

Using the amount of slip we assigned to the Northridge Hills fault from the Trishear model, and the ages used by Tsutsumi and Yeats (1999), we resolve a slip rate of 0.4–2 mm/yr, which agrees with prior estimates. However, if the Mission Hills fault evolved later, than this is also a minimum rate. The observation of folding of young surficial deposits across the Northridge Hills fault led Baldwin et al. (2000) to speculate that the fault exhibits secondary deformation during large magnitude earthquakes. Our structural analysis supports the idea that the north dipping faults are connected (Fuis et al., 2003; Langenheim et al., 2011) and that the shortening is distributing slip onto at least the two main faults, the Mission Hills and Northridge Hills faults. However, due to the observed activity on the Northridge Hills fault at depth (Woods and Seiple, 1995), both primary and secondary deformation should be considered for this fault system.

In the literature, there are two explanations for the formation of the Sylmar basin. Tsutsumi and Yeats (1999) suggested that a fault propagation fold related to the blind, south-dipping Northridge fault might be the cause to the thick sediment accumulation in the Sylmar basin. Langenheim et al. (2011) proposed that the deeply buried Miocene Verdugo-Canyon fault played a role in the formation of the basin. Our model supports the latter hypothesis that the Sylmar basin was formed during the Miocene due to normal faulting. Without initially slipping the normal faults, including the Mission Hills fault, we could not reproduce the observed stratigraphic relief or structure. This demonstrates how an inverted Mission Hills fault should also be considered as a fault that was active in the Miocene.

The Monterey Formation was deposited north of the Santa Susana fault and west of the Sylmar basin, but the lithology north of the Hospital fault does not allow us to determine if the Hospital fault was active as a normal fault during the Miocene. Furthermore, the unconformity between the Towsley Formation and basement rocks makes it difficult to determine how much reverse slip the Hospital fault accommodated because this contact does not match the stratigraphy to the south. The depth of sediments in the Sylmar basin is between 5 and 8 km (Langenheim et al., 2011); such a thick sedimentary column requires either the Monterey Formation to be much thicker than it is south of Mission Hills or that there was preservation of old strata beneath the Miocene section. Therefore, our interpretation of normal faulting extending north of the Leadwell fault system, at least to the edge of the basin or even into it, seems very plausible. It is possible, as demonstrated by our model, that east of the northeastern step of the Santa Susana fault, that the Mission Hills fault was active as a normal fault during the Miocene.

SUMMARY

Our proposed model for the structural evolution of the Sylmar basin demonstrates the likely connectivity of the north dipping reverse and thrust faults in the subsurface, and helps explain how slip can be distributed from the Santa Susana/Hospital/Sierra Madre fault system to the Mission Hills and Northridge Hills faults south of it. Out of sequence slip should not be ruled out and additional investigation on the local age of the Saugus Formation may help constrain the wide range of estimated slip rates. However, the line of evidence we included in combination with our interpretation of regional pattern of southward migration of the locus of deformation along the Western and Central Transverse Ranges, as demonstrated by our forward model, supports the lower estimates (<<1 mm/yr) for the current activity of the Santa Susana fault, with higher rates on the Mission Hills and possibly the Northridge Hills faults.

DATA AVAILABILITY STATEMENT

The raw data supporting the conclusions of this article will be made available by the authors, without undue reservation.

AUTHOR CONTRIBUTIONS

YL lead the research, conducted the Trishear modeling, wrote the manuscript and prepared the figures. TR participated in all aspects of the research and writing. SM conducted the paleoseismic trenching along with TR, prepared the trench log, and took part in the writing process of the manuscript. AH help during the background research, field geomorphologic observations and took part in the writing process of the manuscript. DR participated in field geomorphologic observations as well as discussions and took part in the writing process of the manuscript.

FUNDING

This research was supported by the Southern California Earthquake Center (SCEC) (Contribution No. 10094). SCEC is funded by NSF Cooperative Agreement EAR-1033462 and USGS Cooperative Agreement G12AC20038. This work was supported by funding from SCEC award numbers 15100 (to DR), 17184 (to DR), 16049 (to TR), and 17024 (to TR).

REFERENCES

Atwater, T. M. (1998). Plate tectonic history of southern California with emphasis on the western transverse ranges and northern channel Islands. *Contrib. to Geol. North. Channel islands, South. Calif. Pacific Sect. Am. Assoc. Pet. Geol.* 45, 1–8. doi:10.1130/DNAG-GNA-N.21

Baldwin, J. N., Kelson, K. I., and Randolph, C. E. (2000). Late Quaternary fold deformation along the Northridge Hills fault, Northridge, California: Deformation coincident with past Northridge Blind-thrust earthquakes and other nearby structures?. *Bull. Seismol. Soc. Am.* 90, 629–642. doi:10.1785/0119990056

Birkeland, P. W. (1984). Soils and geomorphology. Oxford University Press.

Boellstroff, J. D., and Steineck, P. L. (1975). Stratigraphic significance of fission-track ages on volcanic ashes in the marine late Cenozoic of Southern California. *Earth Planet. Sci. Lett.* 27 (2), 143–154. doi:10.1016/0012-821X(75)90023-0

Bull, W. B., and McFadden, L. D. (1977). "Tectonic Geomorphology north and south of the Garlock fault, California," in *Geomorphology in arid regions*. Proceedings 8th Binghamton Symposium in geomorphology, Binghamton, NY, September 23–24, 1977. London: Allen and Unwin, 115–138.

Bull, W. B. (1977). Report No.: 14-08-001-G-394. Tectonic geomorphology of the Mojave desert, US geological survey contract report. Available at: https://catalog.hathitrust.org/Record/102492514/ (Accessed 1976).

Bull, W. B. (1979). Threshold of critical power in streams. *Geol. Soc. Am. Bull.* 90, 453–464. doi:10.1130/0016-7606(1979)90<453:tocpis>2.0.co;2

Bull, W. B. (2008). Tectonic geomorphology of mountains: a new approach to paleoseismology. John Wiley & Sons.

Burgette, R. J., Hanson, A. M., Scharer, K. M., Rittenour, T. M., and Mcphillips, D. (2019). Late Quaternary slip rate of the Central Sierra Madre fault , southern California : implications for slip partitioning and earthquake hazard. *Earth Planet. Sci. Lett.* 1, 1–12. doi:10.1016/j.epsl.2019.115907

Butler, R. W. H. (1987). Thrust sequences. *J. Geol. Soc.* 144, 619–634. doi:10.1144/gsjgs.144.4.0619

Campbell, R. H., Wills, C. J., Irvine, P. J., and Swanson, B. J. (2014). Version 2 Open File Report 2005-1019. Preliminary geologic map of the Los Angeles 30'x 60'quadrangle, southern California. Available at: https://pubs.usgs.gov/of/2005/1019/ (Accessed October 19, 2005).

Crowell, J. C. (1979). The San Andreas fault system through time. *J. Geol. Soc.* 136, 293–302. doi:10.1144/gsjgs.136.3.0293

Davis, T. L., and Namson, J. S., (1998). USGS Cross Section 10. Available at: http://www.davisnamson.com/downloads/USGS.Cross.Section.10.pdf (Accessed November 1998).

Davis, T. L. (2016). "The Santa Susana fault, Aliso Canyon gas storage field, southern California-possible fault rupture hazard, gas well integrity, and regulatory implications," in AAPG Pacific Section and Rocky Mountain Section Joint Meeting, Las Vegas, Nevada, October 2–5, 2016. Available at: http://www.searchanddiscovery.com/abstracts/html/2016/90266ps_rms/abstracts/494.html (Accessed October 5, 2016).

Dibblee, T. W. (1982b). "Geology of the Santa Ynez-Topatopa mountains, southern California," in *Geology and mineral Wealth of the California Transverse ranges*. Editors D. L. Fife and J. H. Minch (Santa Ana, CA: South Coast Geologcal Society, Inc.), 41–56.

Dibblee, T. W. J. (1991). Dibblee Geological Foundation Map DF-33. Geologic map of the san Fernando and van Nuys (north half quadrangles, Los Angeles county, California). Scale 1:24,000. https://ngmdb.usgs.gov/Prodesc/proddesc_217.htm

Dibblee, T. W. (1982a). "Regional geology of the transverse ranges province of southern California," in *Geology and mineral Wealth of the California Transverse ranges*. Editors D. L. Fife and J. A. Minch (Santa Ana: South Coast Geologcal Society, Inc.), 7–26.

DiBiase, R. A., Whipple, K. X., Heimsath, A. M., and Ouimet, W. B. (2010). Landscape form and millennial erosion rates in the San Gabriel Mountains, CA. *Earth Planet Sci. Lett.* 289, 134–144. doi:10.1016/j.epsl.2009.10.036

Erslev, E. A. (1991). Trishear fault-propagation folding. *Geol.* 19, 617–620. doi:10.1130/0091-7613(1991)019<0617:tfpf>2.3.co;2

Field, E. H., Arrowsmith, R. J., Biasi, G. P., Bird, P., Dawson, T. E., Felzer, K. R., et al. 2014). Uniform California earthquake rupture forecast, version 3 (UCERF3)--The time-independent model. *Bull. Seismol. Soc. Am.* 104, 1122–1180. doi:10.1785/0120130164

Fuis, G. S., Clayton, R. W., Davis, P. M., Ryberg, T., Lutter, W. J., Okaya, D. A., et al. (2003). Fault systems of the 1971 San Fernando and 1994 Northridge earthquakes, southern California: relocated aftershocks and seismic images from LARSE II. *Geology* 31, 171–174. doi:10.1130/0091-7613(2003)031<0171:fsotsf>2.0.co;2

Furlong, K. P., and Schwartz, S. Y. (2004). Influence of the mendocino triple junction on the tectonics of coastal California. *Annu. Rev. Earth Planet. Sci.* 32, 403–433. doi:10.1146/annurev.earth.32.101802.120252

Harden, J. W. (1982). A quantitative index of soil development from field descriptions: examples from a chronosequence in central California. Geoderma. 28, 1–28.

Hauksson, E., Jones, L. M., and Hutton, K. (1995). The 1994 Northridge earthquake sequence in California: seimological and tectonic aspects. *J. Geophys. Res.* 100 (12), 335–412. doi:10.1029/95jb00865

Heusser, L. E. (1978). Pollen in Santa Barbara Basin, California: a 12,000-yr record. *Geol. Soc. Am. Bull.* 89, 673–678.

Heusser, L. E. (2000). Rapid oscillations in western North America vegetation and climate during oxygen isotope stage 5 inferred from pollen data from Santa Barbara Basin (Hole 893A). *Palaeogeogr. Palaeoclimatol. Palaeoecol.* 161, 407–421.

Huftile, G. J., and Yeats, R. S. (1995). Convergence rates across a displacement transfer zone in the western transverse ranges, Ventura basin, California. *J. Geophys. Res.* 100, 2043–2067. doi:10.1029/94jb02473

Huftile, G. J., and Yeats, R. S. (1996). Deformation rates across the placerita (Northridge Mw = 6.7 aftershock Zone) and hopper Canyon segments of the western transverse ranges deformation belt. *Bull. Seismol. Soc. Am.* 86.s3–s18.

Hughes, A. (2019). Quaternary structural evolution and seismic hazards of the onshore Ventura basin, southern Calicornia. PhD Thesis. London (UK): Imperial College London.

Hughes, A., Bell, R. E., Mildon, Z. K., Rood, D. H., Whittaker, A. C., Rockwell, T. K., et al. (2020). Three-dimensional structure, ground rupture hazards, and static stress models for complex nonplanar thrust faults in the Ventura Basin, Southern California. *J. Geophys. Res. Solid Earth.* 125, e2020JB019539.

Hughes, A., Rood, D. H., Whittaker, A. C., Bell, R. E., Rockwell, T. K., Levy, Y., et al. (2018). Geomorphic evidence for the geometry and slip rate of a young, low-angle thrust fault: Implications for hazard assessment and fault interaction in complex tectonic environments. *Earth Planet. Sci. Lett* 504, 198–210. doi:10.1016/j.epsl.2018.10.003

Ingersoll, R. V. (2001). Tectonostratigraphy of the santa monica mountains, southern California. *AAPG Pacific Sect. Geology an.* 63–70.

Johnson, K. M., Hammond, W. C., Burgette, R. J., Marshall, S. T., and Sorlien, C. C. (2020). Present-Day and long-term uplift across the western transverse ranges of southern California. *J. Geophys. Res. Solid Earth* 125, e2020JB019672. doi:10.1029/2020jb019672

Keller, E. A., and Pinter, N. (1996). *Active tectonics*. Upper Saddle River, NJ: Prentice Hall.

Keller, E. A., and Rockwell, T. K. (1984). "Tectonic geomorphology, quaternary chronology, and paleoseismicity," in Developments and applications of geomorphology. Springer, 203–239.

Langenheim, V. E., Wright, T. L., Okaya, D. A., Yeats, R. S., Fuis, G. S., Thygesen, K., et al. (2011). Structure of the San Fernando Valley region, California: implications for seismic hazard and tectonic history. *Geosphere* 7, 528–572. doi:10.1130/ges00597.1

Levi, S., and Yeats, R. S. (1993). Paleomagnetic constraints on the initiation of uplift on the Santa Susana fault, western transverse ranges, California. *Tectonics* 12, 688–702. doi:10.1029/93tc00133

Levy, Y., Rockwell, T. K., Shaw, J. H., Plesch, A., Driscoll, N. W., and Perea, H. (2019). Structural modeling of the Western Transverse Ranges: an imbricated thrust ramp architecture. *Lithosphere* 11, 868–883. doi:10.1130/l1124.1

Lindvall, S. C., and Rubin, C. M. (2008). Slip rate Studies along the Sierra Madre–Cucamonga Fault System Using geomorphic and Cosmogenic Surface Exposure age Constraints: Collaborative research with. Central Washington University and William Lettis & Associates, Inc. Available at: https://earthquake.usgs.gov/cfusion/external_grants/reports/03HQGR0084.pdf (Accessed 2008).

Liu, L., Spasojevic, S., and Gurnis, M. (2008). Reconstructing Farallon plate subduction beneath north America back to the late cretaceous. *Science* 322, 934–938. doi:10.1126/science.1162921

Numeric Solutions LLC (2019). Aliso Canyon gas storage facility geologic and geomechanical study. Available at: https://www3.socalgas.com/sites/default/files/2019-03/N19G0036_Aliso.20Studies_v4.pdf (Accessed March 20, 2019).

Lung, R., and Weick, R. J. (1987). Exploratory trenching of the Santa Susana fault in Los Angeles and Ventura counties: US geol. *Surv. Prof. Pap.* 1339, 65–70.

Marshall, S. T., Funning, G. J., Krueger, H. E., Owen, S. E., and Loveless, J. P. (2017). Mechanical models favor a ramp geometry for the Ventura-pitas point fault, California. *Geophys. Res. Lett.* 44, 1311–1319. doi:10.1002/2016gl072289

McFadden, L. D., and Weldon, R. J. (1987). Rates and processes of soil development on Quaternary terraces in Cajon Pass, California. *Geol. Soc. Am. Bull.* 98, 280–293. doi:10.1130/0016-7606(1987)98<280:RAPOSD>2.0.CO;2

Miller, K. G., Kominz, A., Browning, J. V., Wright, J. D., and Mountain, G. S. (2005). The phanerozoic record of global sea-level change. *Science* 310, 1293–1298. doi:10.1126/science.1116412

Mori, J., Wald, D. J., and Wesson, R. L. (1995). Overlapping fault planes of the 1971 san Fernando and 1994 Northridge, California earthquakes. *Geophys. Res. Lett.* 22, 1033–1036. doi:10.1029/95gl00712

Nicholson, C., Sorlien, C. C., Atwater, T., J. C., and Crowell, B. P. (1994). Microplate capture, rotation of the western Transverse Ranges, and initiation of the San Andreas transform as a low-angle fault system. *Geology* 22, 491–495. doi:10.1130/0091-7613(1994)022<0491:mcrotw>2.3.co;2

Nilsen, T. H. (1984). Oligocene tectonics and sedimentation, California. *Sediment. Geol.* 38, 305–336. doi:10.1016/0037-0738(84)90084-8

G. B. Oakeshott (Editor) (1975). San Fernando, California, Earthquake of 9 February 1971. *California Div. Mines Geology* 7.

Petersen, M. D., and Wesnousky, S. G. (1994). Fault slip rates and earthquake histories for active faults in southern California. *Bull. Seismol. Soc. Am.* 84, 1608–1649.

Petroleum Experts Ltd. (2018). MOVE. Available at:https://www.mve.com/ (Accessed January 6, 2018).

Ponti, D. J. (1985). The Quaternary alluvial sequence of the Antelope Valley, California. *Geol. Soc. Am. Spec. Pap* 203, 79–96.

Reed, M. P., Burgette, R. J., Scharer, K. M., Lifton, N. A., and McPhillips, D. (2019). "Assessment OF slip and deformation along the santa susana fault, southern California, using high resolution topography," in *GSA Annual Meeting in 2019*. Arizona, Phoenix: GSA.

Rockwell, T. K. (1983). Soil chronology, geology, and neotectonics of the North Central Ventura Basin, California. PhD Thesis. Santa Barbara (CA): University of California.

Rockwell, T. K. (2000). Use of Soil Geomorphology in Fault Studies. *Quat. Geochronol. Methods Appl.* 4, 273–292.

Rockwell, T. K., Keller, E. A., and Johnson Donald, L. (1985). "Tectonic geomorphology of alluvial fans and mountain fronts near Ventura, California," in Tectonic geomorphology. Proceedings of the 15th Annual Geomorphology Symposium. Allen and Unwin Publishers, 183–207.

Rumelhart, P. E., and Ingersoll, R. V. (1997). Provenance of the upper miocene modelo formation and subsidence analysis of the Los Angeles basin, southern California: implications for paleotectonic and paleogeographic reconstructions. *Bull. Geol. Soc. Am.* 109, 885–899. doi:10.1130/0016-7606(1997)109<0885:potumm>2.3.co;2

Schwartz, D. (2018). Large coherent block versus microplate rotaion of the western transverse ranges: a fresh look at paleomagnetic constraints. MS dissertation. San Diego (CA): University of California.

Scott, K. M., and Williams, R. P. (1978). Erosion and Sediment Yields in the Transverse ranges, Southern California. Geological Survey Professional Paper. US Government Printing Office. Available at: https://doi.org/10.3133/pp1030 (Accessed June 1, 2018).

Shields, K. E. (1977). *Structure of the Northeastern Margin of the San Fernanado Valley*. Los Angeles County, California: Ohio University.

Tennyson, M. E. (1989). Pre-transform early Miocene extension in western California. *Geology* 17, 792–796. doi:10.1130/0091-7613(1989)017<0792:ptemei>2.3.co;2

Tsutsumi, H., and Yeats, R. S. (1999). Tectonic setting of the 1971 sylmar and 1994 Northridge earthquakes in the san Fernando Valley, California. *Bull. Seismol. Soc. Am.* 89, 1232–1249.

Whitcomb, J. H., Allen, C. R., Garmany, J. D., and Hileman, J. A. (1973). San Fernando earthquake series, 1971: focal mechanisms and tectonics. *Rev. Geophys.* 11, 693–730. doi:10.1029/rg011i003p00693

Woods, M. C., and Seiple, W. R. (1995). *The Northridge, California, Earthquake of 17 January 1994*. Sacramento, CA: California Department of Conservation, Division of Mines and Geology.

Wright, T. L. (1991). "Structural geology and tectonic evolution of the Los Angeles Basin, California," in *M 52: Active Margin Basins*. Editor K. T. Biddle (AAPG Special Volumes), 35–134.

Yeats, R. S. (1987). Late cenozoic structure of the Santa Susana fault zone. *US Geol. Surv. Profess. Pap.* 1339, 137–160.

Conflict of Interest: The authors declare that the research was conducted in the absence of any commercial or financial relationships that could be construed as a potential conflict of interest.

APPENDICES

In the Appendices we present the soil description (**Table A1**) and the wells we used for construction of the cross section (**Table A2**).

Table A1 | Soil Description, Mission Hills anticline terrace soil.

Horizon	Depth (cm)	Description
A	0–37	10 YR3/3 m, 4.5/3 d; slightly gravelly Loam texture; moderate, coarse subangular blocky structure; soft to slightly hard dry consistence, slightly sticky and slightly plastic wet consistence; no clay films observed; abrupt, irregular boundary to:
Bt1	37–80	7.5-10 YR4/4 m, 7.5 YR4/6 d; very gravelly Sandy Clay Loam texture; strong, coarse angular block structure; extremely hard dry consistence, very sticky and plastic wet consistence; continuous thick clay films on ped faces and within pores, many moderately thick to thick clay films bridging grains (clay film colors range from 7.5 YR 4/3 to 5/6 m); clear, wavy boundary to:
Bt2	80–160	7.5–10 YR4/4 m, 4/6 d; very gravelly Sandy Loam texture; weak to moderately developed coarse subangular blocky structure; slightly hard dry consistence, slightly sticky and non-plastic wet consistence; continuous, thick clay films lining pores, many thin to thick clay films bridging grains, few thick clay films on ped faces (clay film colors 7.5 YR4/4 & 4/6 m, 10 YR 4/4 m), boundary in bench:
Bench	160–230	Bt2 material exposed in the bench, so the Bt2 is inferred to extend to about 230 cm depth.
BC	230–280+	10 YR4/6 m, 5/6 d; very gravelly Loamy Sand texture; massive breaking to weak, coarse subangular blocky structure; soft dry consistence, non-sticky and non-plastic wet consistence; common thin clay films bridging grains in lams, few thin to moderately thick clay films on clast-matric interfaces; boundary in bench;
Bench	280–335	BC in lower bench; gradual, irregular boundary to:
Cox	335–500+	10 YR5/3 m, 5/4 d; very gravelly Sand texture; massive breaking to weak, medium subangular blocky and single grain structure; soft to loose dry consistence, non-sticky and non-plastic wet consistence; Fe_2O_3 and Mn_2O3 banding (indicating a fluctuating groundwater level); boundary not exposed but expected to be abrupt and smooth over Tm bedrock.

Notes: Field conditions: soil is moist from previous nights' rain. Soil exposure is in a benched trench with 4–5 foot risers. Soil was described over a deep "pit" into Tm, where deposits are thickest. Alluvium is cobbly to boulder alluvium interpreted as fluvial deposits over a strath surface. Capping alluvium may be a debris flow deposit as it is more poorly sorted but contains well-rounded clasts. Clasts are rotted in Bt horizon: Most clasts in the upper part of the profile are easily cut with a scrapper although some show resistance but are cut with difficulty. Most clasts are of granitic composition, with some mafic-rich clasts (basalt? Or dark, fine-grained amphibolite)—interpreted as sourced out of the San Gabriel Mountains.

Table A2 | The list of the wells used for constructing the cross section.

Well number	API	Longitude	Latitude	Source
1	3705974	−118.4479	34.2038	Tsutsumi and Yeats (1999)
2	3721802	−118.4549	34.2577	Tsutsumi and Yeats (1999)
3	3720519	−118.4485	34.2702	Tsutsumi and Yeats (1999)
4	3706330	−118.4563	34.2798	Tsutsumi and Yeats (1999)
5	3705892	−118.4652	34.2833	Davis and Namson (1998)
6	3705449	−118.486	34.2882	Tsutsumi and Yeats (1999)
7	3706034	−118.4666	34.3258	Davis and Namson (1998)